Effects of Thermal Treatment on the Mechanical Properties of Larch (*Larix gmelinii*) and Red Oak (*Quercus rubra*) Wood Cell Walls *via* Nanoindentation

Yan Wu,[a,b,c] Haiqiao Zhang,[a,b] Yang Zhang,[a,b,c,*] Siqun Wang,[b,c,*] Xinzhou Wang,[a,b,c] Deliang Xu,[a,b,c] and Xiang Liu [a,b]

Thermally treated wood is widely used for construction, furniture, and flooring because it has better dimensional stability in outdoor conditions. There is a close relationship between the mechanical properties of thermally treated wood cell walls and the performance of its products. The hardness (*H*) and reduced elastic modulus (E_r) of larch (*Larix gmelinii*) and red oak (*Quercus rubra*) wood cell walls were investigated *via* nanoindentation. The results showed that the larch and red oak wood specimens had different nanomechanical properties. The E_r in the larch wood initially increased with a maximum value of 22.4 GPa at 225 °C, then rapidly decreased after 300 °C with a minimum value of 5.7 GPa at 350 °C. The E_r in the red oak wood appeared to have a mild decline. The *H* in both wood species visibly increased with the thermal treatments due to the reduction of organic wood polymers and the increase of inorganic carbon materials.

Keywords: Mechanical properties; Cell wall; Thermal treatment; Temperature

*Contact information: a: Nanjing Forestry University, Nanjing 210037 P.R. China; b: Co-Innovation Center of Efficient Processing and Utilization of Forest Resources, Nanjing Forestry University, Nanjing 210037, China; c: Center for Renewable Carbon, University of Tennessee, 2506 Jacob Drive, Knoxville, TN, 37996, USA;*Corresponding authors: yangzhang31@126.com; swang@utk.edu*

INTRODUCTION

Wood is a natural, porous substance and a renewable biomaterial. It is characterized by its easy processing, high strength-to-weight ratio, good acoustics, and is wide use in the architecture and furniture fields. However, due to its natural characteristics such as wet swelling, dry shrinkage, anisotropy, *etc*., wood isn't suit be applied in some harsh conditions. Therefore, researchers are developing methods to modify wood to counter these disadvantages.

A thermal treatment is an efficient method to improve the properties of wood. During a thermal treatment, there is a density change in the wood's structure as the temperature increases in an inert gas atmosphere (Vafaeenezhad *et al*. 2013). The cellulose crystalline substance of the thermally treated wood remains at 300 °C but is not detected above 350 °C. The layered cell wall structure in the wood fibers and parenchyma cells are retained below 300 °C, but they change to an amorphous-like structure without the layering above 350 °C, as observed with scanning electron microscopy (SEM) (Kwon *et al*. 2009). The thermal treatment of wood at high temperatures can reduce its hygroscopicity without the use of chemicals, while also improving its dimensional stability and resistance to biological degradation (Oumarou *et al*. 2014). An observation of the pyrolysis of nine wood specimens showed only a small change in the nanostructure of the cellulose microfibrils in the bulk wood specimen below 250 °C. The cellulose fibril structure was completely degraded in the bulk wood specimens between 250 °C and 315 °C, and nanometer-sized

inhomogeneities appeared and developed in the pyrolyzed wood specimens above 315 °C (Smith *et al*. 2012). Garcia *et al.* (2008) found that thermal treatment increased the contact angles and decreased the water absorption of wood. Additionally, wicking was reduced approximately 70% to 80% when the wood fibers were treated at 150 °C or 180 °C for 15 min, 30 min, or 60 min. Below 300 °C, the amorphous hemicellulose and cellulose regions were degraded, and the crystallinity of the torrefied biomass increased (Chang *et al*. 2012). The char prepared at 300 °C was primarily composed of lignin and cellulose residues. The carbohydrates were completely lost in the char produced at 350 °C, and most of the lignocellulosic features that consisted predominantly of aromatic structures were lost at 400 °C (Cao *et al*. 2012). The lignin content decreased and both the degree of lignin oxidation and the amount of highly condensed black carbon moieties increased as the temperature increased during the biomass transformation (Wiedner *et al*. 2013). More structurally complicated biochars form between 250 °C and 350 °C, displaying relatively slow sorption rates (Chen *et al*. 2012).

The nanoindentation technique is a useful method to determine the reduced elastic modulus (E_r) and hardness (H) of wood cell walls (Gindl *et al*. 2002; Gacitua *et al*. 2007; Jakes *et al*. 2008; Wang *et al.* 2019). It can also be used to measure the mechanical properties of cell walls of the stalks of crops, including cotton, soybean, rice straw, wheat straw (Wu *et al*. 2010), silver grass (Liao *et al*. 2012), bamboo (Wang *et al*. 2013), hemp stalk (Li *et al*. 2013), and castor stalk (Li *et al*. 2014). Nanoindentation is widely used for measuring micro-scale mechanical properties of materials that are relatively isotropic in their elastic properties, and addressing whether the modulus measured in an indentation test represents that of some specific crystallographic direction or some average value is not an issue. In contrast, some materials have complex hexagonal crystal structures, and because of this, results from these materials can be used to provide some insight into the importance of elastic anisotropy (Oliver and Pharr 1992). According to previous studies, the microstructure and the cell wall properties of red oak (*Quercus rubra*) change dramatically when the carbonization temperature reaches 325 °C. However, research has not been conducted on changes to the mechanical properties (Xu *et al*. 2017).

The objective of this research was to investigate the cell wall mechanical properties of larch (*Larix gmelinii*) and red oak (*Q. rubra*) woods at different thermally treated temperatures (from 200 °C to 400 °C under a nitrogen atmosphere for 10 min) using the nanoindentation technique. The results provided test data and a basic theory for investigating the change regulation of the cell wall mechanical properties for thermally treated wood at a higher temperature for a shorter time.

EXPERIMENTAL

Materials

Specimen preparation

Two different wood species were used as the experiment specimens, larch (*L. gmelinii*) as a representative softwood and red oak (*Q. rubra*) as a hardwood. The larch wood was from the Hei Longjiang Province of P. R. China, and the red oak was from Knoxville, TN, USA. Each wood specimen was taken from the 35th growth ring and was cut using a saw to dimensions of 30 mm (L) × 10 mm (W) × 5 mm (T).

Methods

Thermal modification

The larch wood specimens were randomly divided into eight groups, including seven treatment groups and one group defined as the control group. The seven treatment groups were thermalized under nitrogen atmosphere in a tube furnace (Thermo Scientific, Asheville, NC, USA) at 200 °C, 250 °C, 300 °C, 350 °C, 400 °C, 450 °C, and 500 °C. The control group was not thermalized. One group was added later, treated with a temperature of 225 °C to make the set of values of E_r and H more complete. The red oak specimens were divided into two groups, also thermalized under nitrogen atmosphere in a tube furnace. The temperatures were set to 300 °C and 350 °C to compare the results to the red oak specimens. Once the specimens were placed in the stove, the temperature was increased at a rate of 10 °C/min, and the holding time was 10 min when the set temperature was reached. The specimen surfaces were cut with three types of knives (steel knife from microtome (Leica Ultracut E ultramicrotome lkb-2188, Bromma, Sweden), glass, and diamond knives from ultramicrotome (American Optical Co., Scientific Instrument Division, Buffalo, NY, USA)) to obtain a smooth surface. The smooth specimens were conditioned at 21 °C and 60% relative humidity in the nanoindentation test room for at least 24 h before testing.

Content of carbon and oxygen elements

The thermally modified woods were analyzed using scanning electron microscopy and energy dispersive spectrometry (SEM-EDS) (Zeiss Dual Beam SEM instrument; Carl Zeiss AG, Oberkochen, Germany) that tested the carbon and oxygen contents in the wood cell walls under different temperatures.

Nanoindentation test (NI)

A TriboIndenter® system (Hysitron, Inc., Minneapolis, MN, USA) and a Berkovich indenter with a three-sided pyramidal shape were employed to conduct the nanoindentation test. For all experiments, an area-to-depth function was loaded (Oliver and Pharr 1992), and a closed-loop feedback control was used to ensure precise control of the nanoindentation probe when it was under load-controlled modes. Before any tests, the drift monitoring time was set to 40 s to measure the drift of the system.

Every indentation procedure included four steps. First, a set-point force (2 μN) was established between the nanoindentation probe and specimen surface. When the transducer detected the pre-load force, the indentation test was begun. Second, the peak load was set as 400 μN. The load was increased to a peak load at a loading rate of 30 μN/s. Third, the loading was held at 400 μN for 5 s in order to avoid the effect of creep behavior occurring in viscous material when unloading stage (Liu *et al.* 2006). Finally, the unloading was executed at a loading rate of 30 μN/s. The scanning probe microscopy (SPM) assembly in the TriboIndentor® system was capable of accurately positioning the bond line interface. Using a scan size of 40 μm × 40 μm, indent positions were marked on each specimen surface on the SPM image (as shown in Fig. 1); the indentations were implemented and examined by rescanning the image. Only indentations in the middle of the bond line interface layer, including the cell walls (most in S2 layer), were selected as valid data. At least 30 valid indents were selected, to ensure the accuracy of mean values of reduced elastic modulus and hardness.

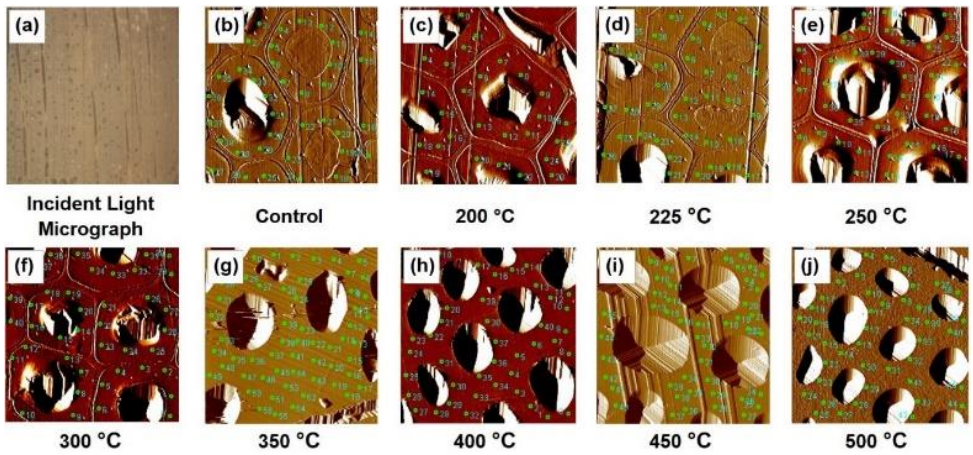

Fig. 1. (a) Incident light micrograph of the transverse section of larch wood specimen; (b) through (j) SPM images of larch wood cell walls after NI at different temperatures

The hardness and reduced elastic modulus were calculated from the valid data following the methods of Oliver and Pharr (1992) and Wu *et al.* (2009). Based on the nanoindentation theory, the E_r was evaluated from the nanoindentation measurements using Eq. 1 (Oliver and Pharr 1992),

$$E_r = \frac{\sqrt{\pi}}{2\beta}\frac{S}{\sqrt{A_{hc}}} \quad (1)$$

where S is the initial unloading rigidity (N/m), β is a correction factor related to the indenter geometry (β = 1.034 for a Berkovich indenter), and A_{hc} is the projected contact area (m^2). The H can be obtained from Eq. 2, where P_{max} is the peak load in this experiment (μN) and A_{hc} is the projected contact area (m^2).

$$H = \frac{P_{max}}{A_{hc}} \quad (2)$$

Creep behavior

The indentation creep ratio (C_{IT}) was introduced to describe the creep behavior, which is defined as the correlative change in indentation depth when the applied load remained constant during the load holding stage. The indentation creep ratio can be measured through Eq. 3, where h_1 and h_2 are the initial and final indentation depths (nm) at the load holding stage, respectively.

$$C_{IT} = \frac{100(h_2 - h_1)}{h_1} \quad (3)$$

RESULTS AND DISCUSSION

Carbon and Oxygen Contents

Figure 2 shows the C and O contents of the larch and red oak woods with different treating temperatures. The carbon contents increased while the oxygen amount decreased with increasing treatment temperatures in both the larch and red oak wood specimens. When the thermally treatment temperature was between 300 °C to 350 °C, the elemental

contents of the larch and red oak wood specimens exhibited consistency in changes due to the chemical composition being carbonized with the increase of temperature.

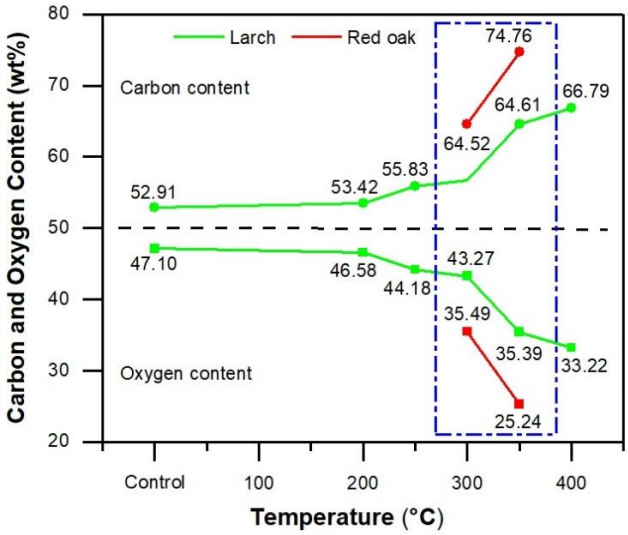

Fig. 2. The tendency of carbon and oxygen contents of larch and red oak wood specimens at different temperatures

Nanoindentation test of *H* and E_r

As previously mentioned, the NI procedure included four steps. Figure 3 and 4 show the load-depth curves and time-depth relationship of the larch wood specimens with different treating temperatures. The values in both curves were randomly selected from experimental data that had invalid data removed. As shown in Fig. 3, the indentation depth at 350 °C was larger than others, the value of h_1 was 232.8 nm, and the value of h_2 was 244.4 nm.

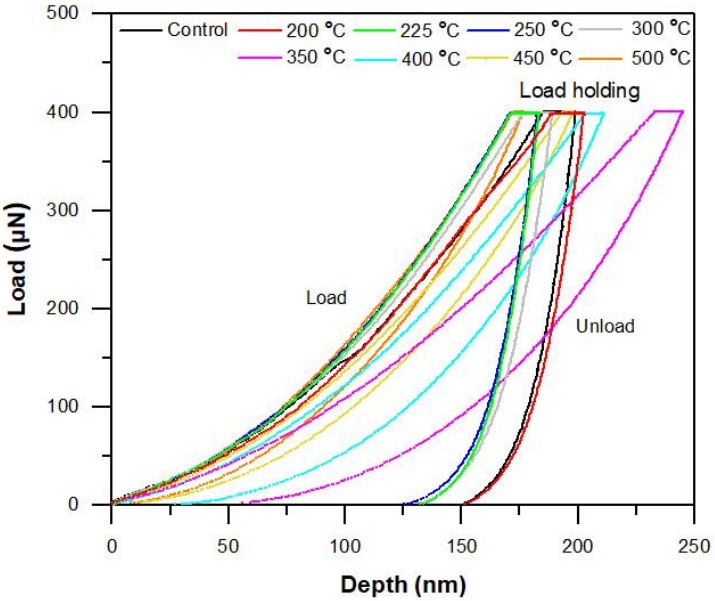

Fig. 3. Load-depth curves of larch wood specimens at different temperatures

Figure 4 shows the general trend of the indentation depth. A rise in the thermal treatment temperature caused the trend to initially increase and then decrease. The h_1 of 500 °C was close to the values at 225 °C and 250 °C, and the h_1 of control group was deeper than these three groups. However, the data at 200 °C did not match the trend, which could have been caused by the random selection of valid data. When the thermal treatment temperature was above 350 °C, the depth of pressing in the load holding stage was gradually reduced from 11.63 nm to 4.24 nm (500 °C), which could also be known from Fig. 4.

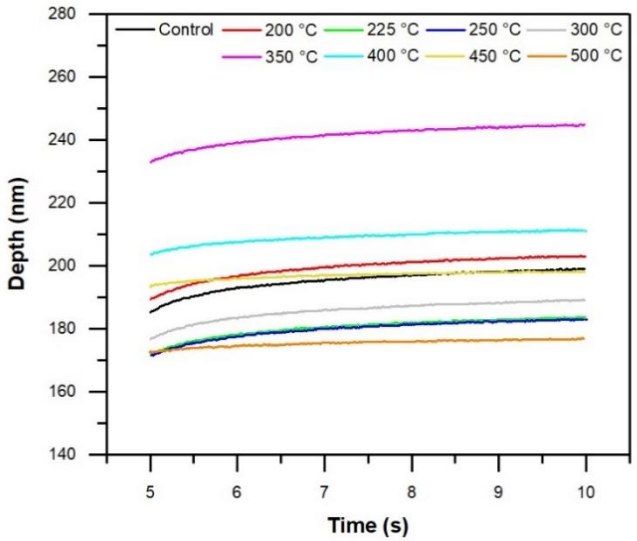

Fig. 4. Time-depth curves of larch wood specimens at different temperatures

The randomly selected valid data concerning E_r and H in the secondary cell walls of the larch and red oak wood is summarized in Fig. 5. The E_r in the larch wood increased with an increased temperature from 200 °C to 225 °C, and the maximum value was 22.4 GPa (at 225 °C). There was a rapid downward trend when the temperature increased to 300 °C and the minimum value was 5.7 GPa. There was a slight increase above 350 °C. However, the E_r of the red oak appeared to have a mild decline from 300 °C to 350 °C. The H value of the larch wood increased with an increased temperature, as shown in Fig. 5.

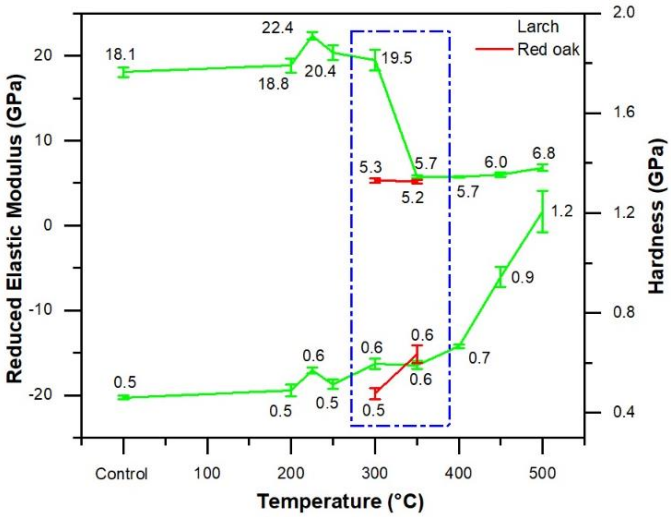

Fig. 5. E_r - temperature and H - temperature curves of larch and red oak wood specimens at different temperatures

The maximum value was 1.21 GPa at 500 °C, which was 163% higher than the control sample. The E_r value decreased while the H value increased with an increasing temperature, which may have contributed to the carbon content increase and the oxygen content decrease in the wood specimens. The layers of wood cell walls disappeared and the structure rendered the uniformity of graphitization when the temperature was as high as 350 °C. This led to remarkable changes of mechanical properties of the thermal-treated wood specimens compared to the control specimens.

Creep Behavior

Figure 6 shows the time-depth curves of the larch wood at different thermal treatment temperatures. The creep behavior of wood is a vital performance index, particularly when large wooden structures are submitted to long-term loading. The effects of thermal modification on the creep behavior of the cell walls were analyzed after the load holding stage.

As shown in Fig. 6, a gradually decreased tendency of the indentation C_{IT} for the control larch wood specimen (7.51%) when the thermal treatment was 500 °C (2.46%). The red oak specimens at 300 °C and 350 °C exhibited the same tendency as the larch wood and the values were lower than the larch wood values. Hemicelluloses are key compounds responsible for the time-dependent creeping, as they act as a type of viscous matrix (Wang *et al*. 2018).

The degradation of hemicellulose and cellulose led to the weakening of the flexible connections between the cell wall polymers, which resulted in an elevated creep resistance. The increased carbon content and the decreased oxygen content with increasing temperatures were the major contributors to the elevated creep resistance. The severe thermal treatment (temperatures above 300 °C) for the larch and red oak woods in addition to the lower E_r and higher H values may have contributed to the negative effect on the creep resistance of the thermally treated wood.

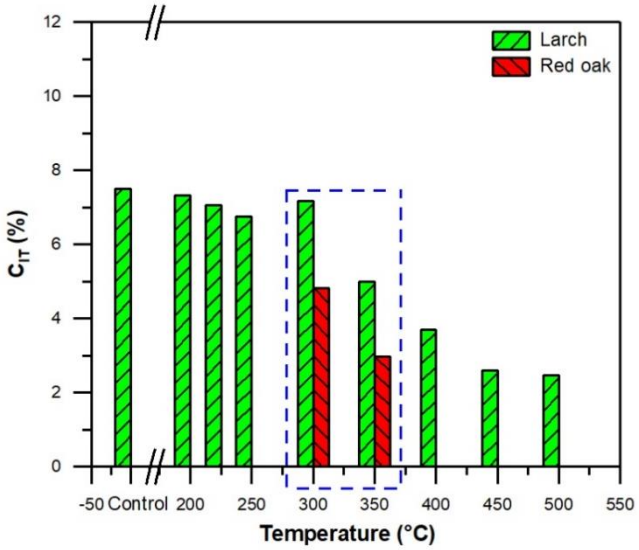

Fig. 6. C_{IT} of larch and red oak wood specimens at different temperatures

CONCLUSIONS

1. A rise in thermal treatment temperatures resulted in an increased carbon element and a decreased oxygen element.
2. The reduced elastic modulus (E_r) and hardness (H) of the larch and red oak wood specimens were different at the same temperature of 300 °C and 350 °C. The E_r decreased and H increased with increasing temperatures, which may have contributed to the increase of carbon content and the decrease of oxygen content in the thermally treated wood specimens.
3. The wood cell wall layers disappeared and the uniformity of graphitization in the structure increased when the temperature was as high as 350 °C, which led to remarkable changes in the mechanical properties of the thermal-treated wood specimens when compared to the control.

ACKNOWLEDGMENTS

The authors gratefully acknowledge the financial support of the project funded by the Jiangsu Government Scholarship for Overseas Studies, the USDA National Institute of Food and Agriculture (Hatch Project 1012359), the Postgraduate Research & Practice Innovation Program of Jiangsu Province (KYCX17-0828), and the Huzhou, Zhejiang province "Nan Taihu Lake elite plan" project ([2018] No.2). The authors thank Mr. Chris Helton and Professor David Harper in the Center for Renewable Carbon at University of Tennessee for their kind help of the sample preparation and data analysis, respectively.

REFERENCES CITED

Cao, X., Pignatello, J. J., Li, Y., Lattao, C., Chappell, M. A., Chen, N., Miller, L. F., and Mao, J. (2012). "Characterization of wood chars produced at different temperatures using advanced solid-state ^{13}C NMR spectroscopic techniques," *Energ. Fuel.* 26(9), 5983-5991. DOI: 10.1021/ef300947s

Chang, S., Zhao, Z., Zheng, A., He, F., Huang, Z., and Li, H. (2012). "Characterization of products from torrefaction of sprucewood and bagasse in an Auger reactor," *Energ. Fuel.* 26(11), 7009-7017. DOI: 10.1021/ef301048a

Chen, Z., Chen, B., and Chiou, C. T. (2012). "Fast and slow rates of naphthalene sorption to biochars produced at different temperatures," *Environ. Sci. Technol*. 46(20), 11104-11111. DOI: 10.1021/es302345e

Gacitua, W. E., Ballerini, A. A., Lasserre, J. P., and Bahr, D. (2007). "Nanoindentation and ultrastructure in *Eucalyptus nitens* with micro and mesocracks," *Maderas- Cienc. Tecnol.* 9(3), 259-270. DOI: 10.4067/S0718-221X2007000300006

Garcia, R. A., Riedl, B., and Cloutier, A. (2008). "Chemical modification and wetting of medium density fibreboard produced from heat-treated fibres," *J. Mater. Sci.* 43(15), 5037-5044. DOI: 10.1007/s10853-008-2596-z

Gindl, W., Gupta, H. S., and Grünwald, C. (2002). "Lignification of spruce tracheid secondary cell walls related to longitudinal hardness and modulus of elasticity using nano-indentation," *Can. J. Botany* 80(10), 1029-1033. DOI: 10.1139/B02-091

Jakes, J. E., Frihart, C. R., Beecher, J. F., Moon, R. J., and Stone, D. S. (2008). "Experimental method to account for structural compliance in nanoindentation measurements," *J. Mater. Res.* 23(4), 1113-1127. DOI: 10.1557/JMR.2008.0131

Kwon, S. M., Kim, N. H., and Cha, D. S. (2009). "An investigation on the transition characteristics of the wood cell walls during carbonization," *Wood Sci. Technol.* 43(5-6), 487-498. DOI: 10.1007/s00226-009-0245-6

Li, X. P., Du, G. B., Wang, S. Q., and Yu, G. (2014). "Physical and mechanical characterization of fiber cell wall in castor (*Ricinus communis* L.) stalk," *BioResources* 9(1), 1596-1605. DOI: 10.15376/biores.9.1.1596-1605

Li, X. P., Wang, S. Q., Du, G. B., Wu, Z., and Meng, Y. J. (2013). "Variation in physical and mechanical properties of hemp stalk fibers along height of stem," *Ind. Crop. Prod.* 4, 344-348. DOI: 10.1016/j.indcrop.2012.05.043

Liao, C., Deng, Y., Wang, S., Meng, Y., Wang, X., and Wang, N. (2012). "Microstructure and mechanical properties of silvergrass fibers cell evaluated by nanoindentation," *Wood Fiber Sci.* 44(1), 63-70. DOI:

Liu, C. K., Lee, S., Sung, L. P., and Nguyen, T. (2006). "Load-displacement relations for nanoindentation of viscoelastic materials," *J. Appl. Phys.* 100(3), Article ID 033503. DOI: 10.1063/1.2220649

Oliver, W. C., and Pharr, G. M. (1992). "An improved technique for determining hardness and elastic modulus using load and displacement sensing indentation experiments," *J. Mater. Res.* 7(6), 1564-1583. DOI: 10.1557/JMR.1992.1564

Oumarou, N., Kocaefe, D., and Kocaefe, Y. (2014). "3D-modelling of conjugate heat and mass transfers: Effects of storage conditions and species on wood high temperature treatment," *Int. J. Heat Mass Tran.* 79, 945-953. DOI: 10.1016/j.ijheatmasstransfer.2014.08.086

Smith, A. J. MacDonald, M. J. Ellis, L. D. Obrovac, M. N., and Dahn, J. R. (2012). "A small angle X-ray scattering and electrochemical study of the decomposition of wood during pyrolysis," *Carbon* 50(10), 3717-3723. DOI: 10.1016/j.carbon.2012.03.045

Vafaeenezhad, H., Zebarjad, S. M., and Vahdati, K. J. (2013). "Intelligent modeling using fuzzy rule-based technique for evaluating wood carbonization process parameters," *The International Journal of Advanced Manufacturing Technology* 68(5-8), 1471-1478. DOI: 10.1007/s00170-013-4935-8

Wang, H., Wang, H., Li, W., Ren, D., and Yu, Y. (2013). "Effects of moisture content on the mechanical properties of moso bamboo at the macroscopic and cellular levels," *BioResources* 8(4), 5475-5484. DOI: 10.15376/biores.8.4.5475-5484

Wang, X., Chen, X., Xie, X., Wu, Y., Zhao, L., Li, Y., and Wang, S. (2018). "Effects of thermal modification on the physical, chemical and micromechanical properties of Masson pine wood (*Pinus massoniana* Lamb.)," *Holzforschug* 72(12), 1063-1070. DOI: 10.1515/hf-2017-0205

Wang, X., Chen, X., Xie, X., Cai S., Yuan Z., and Li Y. (2019). "Multi-scale evaluation of the effect of phenol formaldehyde resin impregnation on the dimensional stability and mechanical properties of *Pinus massoniana* Lamb.," *Forests* 10(8), article nol. 646. DOI: 10.3390/f10080646

Wiedner, K., Naisse, C., Rumpel, C., Pozzi, A., Wieczorek, P., and Glaser, B. (2013). "Chemical modification of biomass residues during hydrothermal carbonization – What makes the difference, temperature or feedstock?," *Org. Geochem.* 54, 91-100. DOI: 10.1016/j.orggeochem.2012.10.006

Wu, Y., Wang, S., Zhou, D., Xing, C., Zhang, Y., and Pharr, G. M. (2009). "Use of nanoindentation and SilviScan to determine the mechanical properties of 10 hardwood species," *Wood Fiber Sci.* 41(1), 64-73. DOI:

Wu, Y., Wang, S., Zhou, D., Xing, C., Zhang, Y., and Cai, Z. (2010). "Evaluation of elastic modulus and hardness of crop stalks cell walls by nanoindentation," *Bioresource Technol.* 101(8), 2867-2871. DOI: 10.1016/j.biortech.2009.10.074

Xu, D. L., Ding, T., Li, Y. J., Zhang, Y., Zhou, D. G., and Wang, S. Q. (2017). "Transition characteristics of a carbonized wood cell wall investigated by scanning thermal microscopy (SThM)," *Wood Sci. Technol*. 51(4), 831-843. DOI: 10.1007/s00226-017-0919-4

Article submitted: May 2, 2019; Peer review completed: August 4, 2019; Revised version received and accepted: August 14, 2019; Published: August 21, 2019.
DOI: 10.15376/biores.14.4.8048-8057